Supporting Information

Yamaguchi et al. 10.1073/pnas.1307185110

SI Materials and Methods

Reagent for Flow Cytometric Analysis. The following reagents were purchased from BD Biosciences: anti-CD4 (RM4-5), anti-CD8a (53-6.7), anti-CD11c (HL3), anti-CD25 (PC61), anti-CD40 (3/23), anti-CD80 (16-10A1), anti-CD86 (GL1), anti-I-A^d (MHC class II; AMS-32.1), anti-Thy1.1 (OX-7), anti-Thy1.2 (53-2.1), anti-lymphocyte function-associated antigen-1 (LFA-1; M17/4), anti-intercellular adhesion molecule-1 (ICAM-1; 3E2), anti-DO11.10 T-cell receptor (TCR) (KJ-1.26), anti–TCR-Vβ2 (B20.6), Vβ3 (KJ25), Vβ5 (MR9-4), Vβ6 (RP4-7), Vβ8.1/8.2 (MR5-2), Vβ8.3 (1B3.3), Vβ11 (RR3-15), Vβ12 (MR11-1), Vβ14 (14-2), anti-cytotoxic T lymphocyte-associated antigen 4 (CTLA-4; UC10), anti–Ki-67 (35), anti–IL-4 (11B11), anti–IFN-γ (XMG1.2), and control IgG. Anti-forkhead box p3 (Foxp3; FJK-16s) was purchased from eBioscience.

Suppression Assay with Human T Cells. ***Lentiviral constructs, production, and concentration.*** Reagents for production of lentivirus (BLOCK-iT Lentiviral Pol II miR RNAi Expression System with EmGFP for RNAi analysis and pLenti6/V5 Directional TOPO Cloning Kit for exogenous gene transduction) were purchased from Invitrogen. To knockdown human IL-2, artificial microRNA sequences were purchased from BLOCK-iT miR RNAi Select (Invitrogen). The DNA fragments for the microRNAs were inserted into the lentiviral vector pLenti6/V5 with GFP. To prepare lentivirus with human CTLA-4, the human *CTLA-4* gene was inserted into retroviral plasmid pGCSamIN (a gift from M. Onodera, Tsukuba University, Tsukuba, Japan), which contained internal ribosome entry site (IRES) and human truncated nerve growth factor receptor (NGFR). DNA fragments encoding human CTLA-4-IRES–NGFR were inserted into pLenti6/V5 TOPO vector. The pLenti6/V5 vectors containing DNA fragments for microRNAs or the *CTLA-4* gene were cotransfected into the 293FT cell line (Invitrogen) with the ViraPower Packaging Mix to produce lentivirus. Forty-eight hours after transfection, supernatant was collected by centrifugation at 3,000 × *g* for 10 min, filtered through a 0.45-μm filter (Millipore), and subjected to ultracentrifugation at 50,000 × *g* at 4 °C for 2 h (HITACHI-koki himac). The resulting lentivirus-containing medium was >70-fold concentrated and stored at −80 °C until use. One milliliter of the viral stocks could transduce genes into more than 1×10^7 293FT cells.

Lentiviral transduction into primary human T lymphocytes. $CD25^-CD45RA^+CD4^+$ naive T cells were sorted with MoFlo from peripheral blood mononuclear cells (PBMCs) of healthy volunteers. To infect with lentivirus, sorted naive T cells were activated using Dynabeads Human T-Activator CD3/CD28 (Invitrogen) and adding 50 IU/mL human IL-2 every other day. Four days later, activated T cells were virus-infected by centrifuging at 1,000 × *g*, 32 °C, for 90 min in the presence of lentivirus (Virus number/target cell number was more than 10), 8 μg/mL polybrene (Millipore), 200 IU/mL IL-2, and Dynabeads CD3/CD28 and by incubating for 6 h at 37 °C. On the following day, viral infection was repeated in the same way; and on the next day, infected cells were sorted with MoFlo as GFP- and NGFR-positive cells to prepare CTLA-4–transduced and knocked down IL-2 cells.

Suppression assay with human T cells. CFSE-labeled responder $CD25^-CD45RA^+CD4^+$ T cells (1×10^4) were cocultured with graded numbers of $CD25^{high}CD4^+$ Treg cells or activated T cells with or without virus infection in the presence of 2×10^3 nonirradiated allogeneic monocyte-derived DCs and 0.5 μg/mL plate-bound anti-CD3 (OKT3) in 96-well round-bottom plates. Four days later, collected cells were stained with anti-CD4 and anti-Foxp3 and analyzed with Canto II. To generate monocyte-derived dendritic cells (DCs), $CD14^+$ monocytes were positively sorted from PBMCs by magnet sorting using magnetic beads–conjugated anti-CD14 (Milteny Biotec). Sorted $CD14^+$ cells were cultured in six-well plates with 50 ng/mL of recombinant GM-CSF (PeproTech) and 20 ng/mL of IL-4 (PeproTech); 6 d later, cultured cells were harvested and used as monocyte-derived DCs, which were negative for CD14 and positive for CD11c, CD80, and CD86.

TCR Repertoire Analysis by Sequencing the CDR3 Region. For sequencing of TCRJα, CDR3 regions with TCRVα10 were amplified from CD4SP thymocytes expressing DO11.10 transgenic TCR Vβ. Thymocytes were stained with phycoerythrin-cyanin 7 (PE-Cy7)–conjugated anti-CD8, and then $CD8^+$ cells were depleted by panning with goat anti-rat IgG antibody–coated dishes (MP Biomedicals). The crude $CD8^-$ cells were further stained with antibodies specific for CD25, CD4, CD8, KJ-1.26, and TCRVβ8.1/8.2. Among the $CD4^+CD8^-KJ1.26^{low}$ $TCRVβ8^+$ fraction, $CD25^+$ and $CD25^-$ cells were sorted with MoFlo. From the lysates of sorted cells, RNA was purified with RNAeasy (QIAGEN), and cDNA was prepared with random primers and reverse transcriptase III (Invitrogen). TCR Vα10–containing fragments were amplified with nested PCR using a Vα10-specific primer (GACTCGTCAGCCTGTTCTACAATC) and common Vα primer (CACAGGGAACGTCTGAACTG) in the first PCR and the Vα10-specific primer (GACTCGTCAGCC-TGTTCTACAATC) and another common Vα primer (ACAC-AGCAGGTTCTGGGTTC) in the second PCR. Amplified fragments were inserted into TA-cloning vector (Invitrogen) and transformed into *Escherichia coli* (DH-5α; TOYOBO), and colonies were picked up. The DNA sequence of amplified PCR products including the TCRJα region were determined with a DNA sequencer (3130X/Genetic Analyzer; Applied Biosystems) and analysis software (Genetyx) referring to the *TCRa* sequence in National Center for Biotechnology Information (NCBI). Ninety-eight, 85, and 83 different sequences were determined from WT $CD25^-$CD4SP thymocytes, WT $CD25^+$CD4SP thymocytes, and $CD25^-$CD4SP thymocytes from IL-2 gene KO (IL2KO)-C4Tg mice, respectively, by more than nine independent PCR amplifications from four mice per group. The determined J segments had at least 85% similarity to a particular TCR Jα segment in the genome. TCR Jα segments which occupy at least 3% as mean frequency or 5% as maximum frequency among the three populations are shown in Fig. S6*B*, and their correlation coefficienct was calculated.

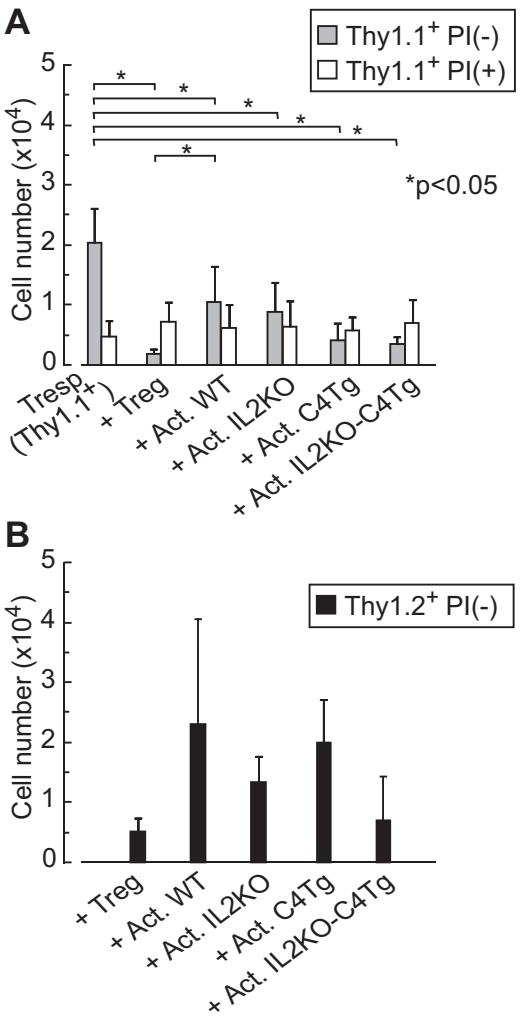

Fig. S1. Effects of suppressive T cells on the number of live or dead responder T cells. The number of propidium iodide (PI)-negative or PI-positive $CFSE^+$ $Thy1.1^+$ $CD25^-CD4^+$ responder T cells (Tresp) cells (*A*) and PI-negative $Thy1.2^+$ cells (*B*) of indicated cell populations were analyzed after 3-d culture at 1:1 ratio as shown in Fig. 4*B*. The mean ± SD of four independent experiments is shown. One-way ANOVA followed by Tukey-Kramer's posttest was used to analyze the difference.

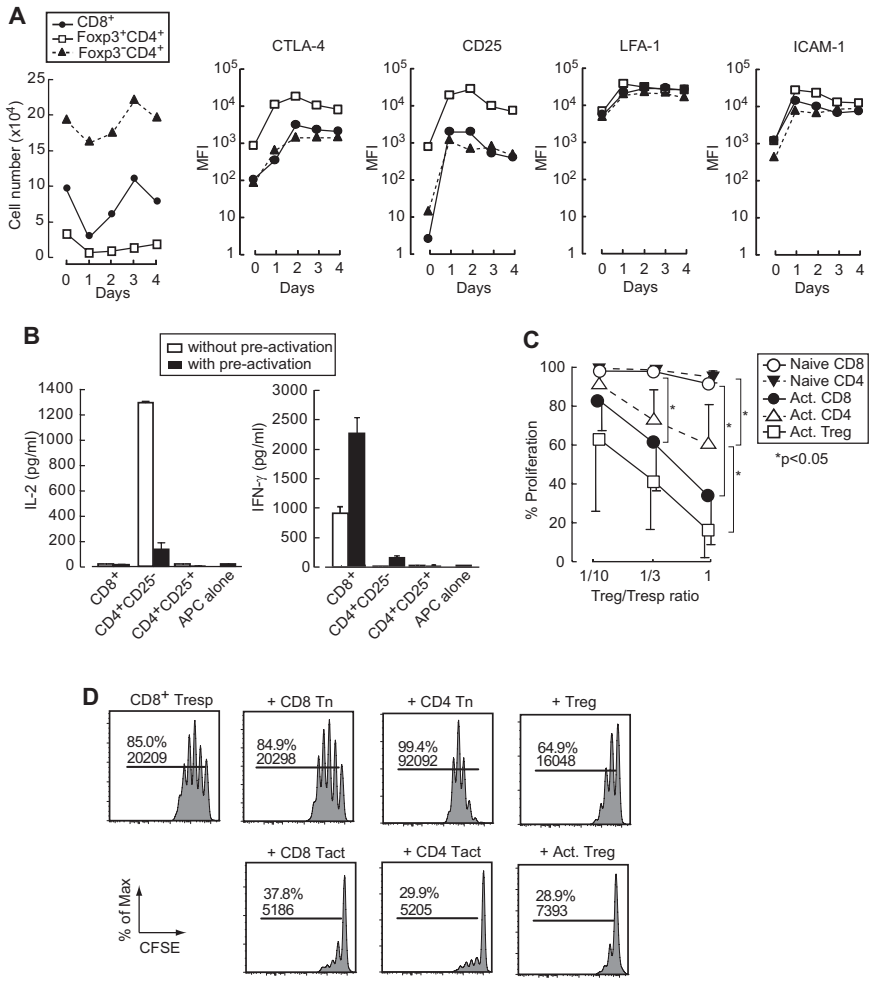

Fig. S2. Suppressive activity of conventional activated CD8$^+$ T cells. (*A*) Cell numbers and expression levels of intracellular CTLA-4 and cell surface CD25, LFA-1, and ICAM-1 (CD54) were compared among lymph node cell populations (CD8$^+$, Foxp3$^+$CD4$^+$, and Foxp3$^-$CD4$^+$ T cells) during in vitro activation for 4 d. Lymph node cells from Foxp3 reporter mice were stimulated with anti-CD3. (*B*) IL-2 and IFN-γ concentration (mean ± SD of triplicates) assessed by ELISA in the culture supernatants after 3-d culture. (*C*) Proliferation of Thy1.1$^+$CD25$^-$CD4$^+$ Tresp cells cocultured with graded numbers of designated populations of Thy1.2$^+$ cells. Proportions of dividing Tresp cells were normalized by the proliferation of Tresp cells alone. The means ± SDs of three independent experiments are shown. Act., preactivated. *$P < 0.05$ indicates significant difference in post hoc comparison for ANOVA. (*D*) CFSE intensity of dividing CFSE-labeled Thy1.1$^+$ CD8$^+$ Tresp cells cocultured with the same number of designated T-cell populations. Representative results of three independent experiments are shown in *A*, *B*, and *D*. The results show that activated CD8$^+$ T cells and, to a lesser extent, activated CD4$^+$ T cells exhibit significant in vitro suppressive activity when they cease IL-2 production but still express CTLA-4 (e.g., 3 d after in vitro anti-CD3 stimulation).

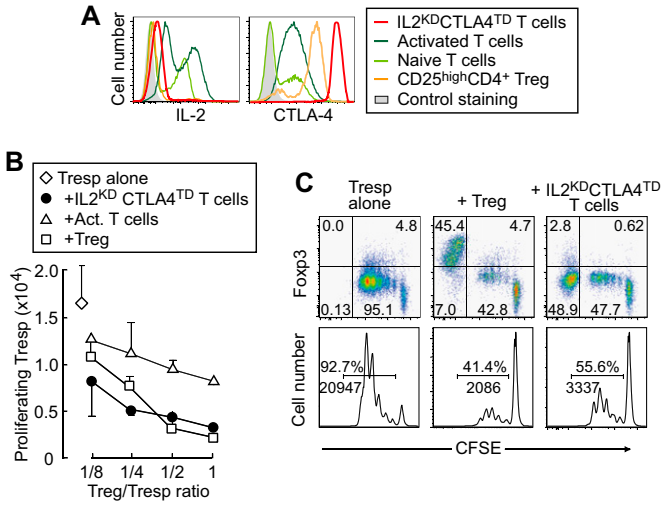

Fig. S3. Suppressive activity of IL-2 knockdown and CTLA-4–transduced human CD4$^+$ T cells. (*A*) Intracellular IL-2 and CTLA-4 expression by indicated human CD4$^+$ T cells after stimulation with phorbol 12-myristate 13-acetate (PMA) and ionomycin. CD25$^-$CD45RA$^+$CD4$^+$ naive T cells and CD25^{high}CD4$^+$ Treg cells were sorted from human peripheral blood. IL2^{KD}CTLA4^{TD} T cells indicate IL-2 knockdown and CTLA-4–transduced activated CD4$^+$ T cells, which were derived from CD25$^-$CD45RA$^+$CD4$^+$ naive T cells, activated with anti-CD3 and anti-CD28, and infected with lentivirus expressing siRNA against *IL-2* and mRNA for *CTLA-4*. (*B*) The number of proliferating CFSE-labeled human CD25$^-$CD45RA$^+$CD4$^+$ naive Tresp cells in the presence of graded numbers of indicated populations. (*C*) CFSE and Foxp3 expression by CD4$^+$ T cells (*Upper*) and CFSE intensity of CFSE$^+$ CD4$^+$ T cells (*Lower*) are shown with the percentages (*Upper* and *Lower*) and cell numbers (*Lower*) in gated areas. Results are representative of three independent experiments.

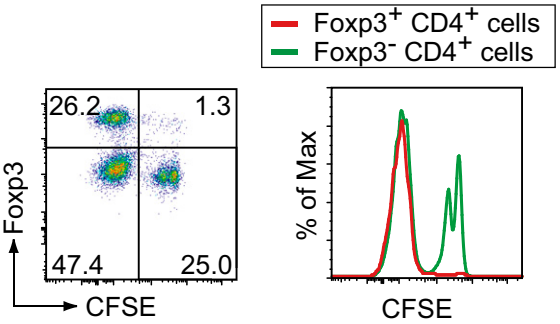

Fig. S4. Proliferation of Foxp3$^+$ Treg cells in RAG2$^{-/-}$ mice. CFSE-labeled CD4$^+$ T cells (1×10^6) were transferred into RAG2$^{-/-}$ mice and CD4$^+$TCRβ$^+$ T cells in inguinal lymph nodes were stained 7 d later for CFSE and Foxp3 (*Left*). CFSE staining of Foxp3$^+$CD4$^+$TCRβ$^+$ cells and Foxp3$^-$CD4$^+$TCRβ$^+$ cells is shown on *Right*. Numbers indicate the percentages in gated areas. Representative of three independent experiments.

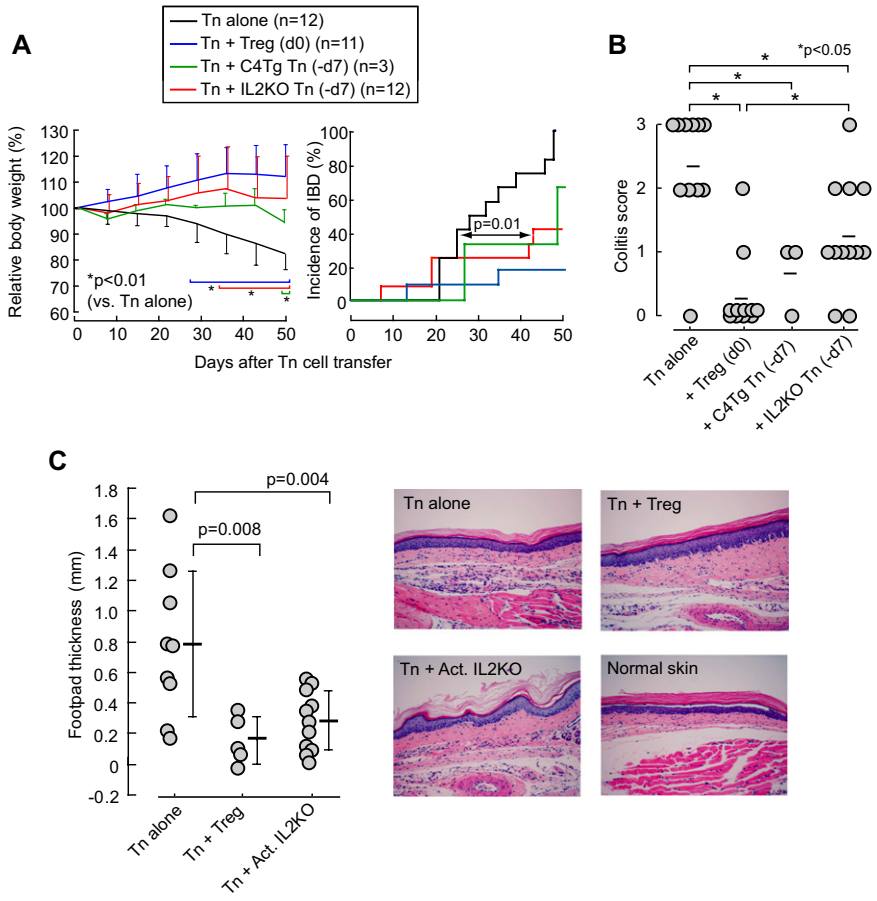

Fig. S5. In vivo suppressive activity of IL-2KO T cells. (*A* and *B*) Suppression of colitis in RAG2$^{-/-}$ mice by pretransfer of C4Tg and IL2KO T cells. (*A*) Body weight change (mean ± SD) (*Left*) and incidence of IBD (*Right*) depicted as diarrhea in RAG2$^{-/-}$ mice transferred with WT CD45RB^{high}CD4^{+} Tn cells alone on day 0 (black lines), WT CD25^{+}CD4^{+} Treg cells and WT CD45RB^{high}CD4^{+} Tn cells on day 0 (blue lines), C4Tg CD45RB^{high}CD25^{-}CD4^{+} T cells 7 d earlier (–d7) and WT CD45RB^{high}CD4^{+} Tn cells on day 0 (green lines), or IL2KO CD45RB^{high}CD25^{-}CD4^{+} T cells 7 d earlier (–d7) and WT CD45RB^{high}CD4^{+} Tn cells on day 0 (red lines). Cell dose was all 1×10^5. (*B*) Histological score of colitis in each group of recipient mice. Horizontal bars indicate the means. Data are pooled from seven independent experiments. *$P < 0.05$ indicates significant difference in post hoc comparison for ANOVA. (*C*) Suppression of delayed type hypersensitivity reaction by activated IL2KO T cells. Athymic BALB/*c* nude mice were transferred with 1×10^6 CD25^{-}CD4^{+} naïve T cells from DO11.10 TCR transgenic mice together with the same numbers of CD25^{+}CD4^{+} Treg cells from DO11.10 mice or preactivated CD4^{+} T cells from DO11.10 IL2KO mice. On the same day, mice were immunized by s.c. injection of 100 μg ovalbumin (OVA) protein emulsified in 50 μL complete Freund's adjuvant; 7 d later, 100 μg OVA protein in PBS was injected into right footpad of the immunized nude mice; and thickness of food pads was measured 24 h later. The preactivated IL2KO CD4^{+} T cells were prepared from lymph nodes and spleens of DO11.10 IL2KO RAG2$^{-/-}$ mice by stimulation with OVA$_{322–339}$ peptide and 100 U/mL of IL-2 for 4 d. Each dot indicates the difference of thickness between immunized right footpad and left footpad in each mouse. Bars indicate mean ± SD. Representative H&E-stained histology of footpads is also shown.

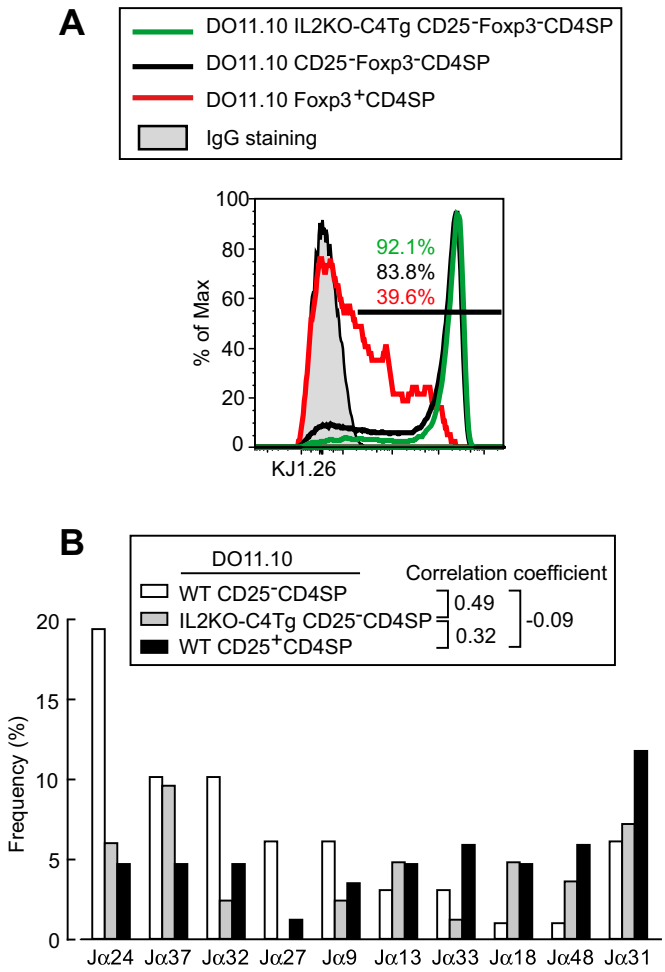

Fig. S6. CTLA-4–dependent self-skewing of TCR repertoire in developing T cells. (*A*) Staining of DO11.10 Foxp3$^+$ or CD25$^-$Foxp3$^-$ CD4SP thymocytes and DO11.10 IL2KO-C4Tg CD25$^-$Foxp3$^-$ CD4SP thymocytes with KJ1.26, an antibody specific for the DO11.10 transgenic TCR clonotype. (*B*) Proportions of thymocytes using indicated TCR Jα among CD4SP thymocyte populations (IL2KO-C4Tg CD25$^-$, WT CD25$^-$, and WT CD25$^+$) expressing DO11.10 transgenic TCRβ and endogenous TCR Vα10 were evaluated by PCR and sequencing. Summary of nine experiments is shown with correlation coefficients in *Inset*.

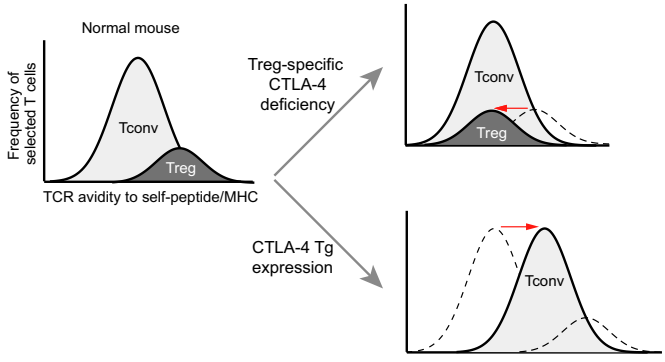

Fig. S7. Effect of CTLA-4 expression on selection of self-reactive TCR-expressing T cells in the thymus. In normal mice, Treg cells are more self-reactive than conventional T cells in the TCR repertoire. Regulatory T (Treg) cell–specific CTLA-4 deficiency cancels this self-skewing in the Treg TCR repertoire. On the other hand, in CTLA-4 transgenic mice, the TCR repertoire of conventional T cells is skewed to be more self-reactive than in normal mice, whereas Treg cells are not generated, presumably because of marked CD28 signal reduction due to high CTLA-4 expression.

Table S1. Primers list for quantitative PCR analysis

Gene name	Primer sequences
Cd25 (Il2receptorα)	CTGATCCCATGTGCCAGGAA and AGGGCTTTGAATGTGGCATTG
Itgb8 (integrinß8)	ACTTCTCCTGTCCCTATCTCCA and ATCTGCCACCTTCACACTCC
Ctla4 (Cd152)	CCTCTGCAAGGTGGAACTCATGTA and AGCTAACTGCGACAAGGATCCAA
Cd39 (Entpd1)	GCAAGCAGAGACAGCAAAAAC and GCAAAATCTCTTCACCTTAGAATCC
Lag-3 (Cd223)	TCTCCATCACGTACAACCTCA and GCAGCGTACACTGTCAGAGG
Pd-1 (programmed cell death 1)	TGCAGTTGAGCTGGCAAT and GGCTGGGTAGAAGGTGAGG
Galectin-1	CTCTCGGGTGGAGTCTTCTG and GGTTTGAGATTCAGGTTGCTG
Cd73 (Nt5e)	ATGAACATCCTGGGCTACGA and GTCCTTCCACACCGTTATCAA
Icam1 (Cd54)	CAATTCACACTGAATGCCAGCTC and CAAGCAGTCCGTCTCGTCCA
Cd69	GGAAAATAGCTCTTCACATCTGG and TGATGCTTCTCAAAATGTATACTGG
Itgb2 (CD18)	GTGGTGCAGCTCATCAAGAA and GCTGTGGTCCAGGAAGACTC
Fasl (Cd178)	ACCGGTGGTATTTTTCATGG and AGGCTTTGGTTGGTGAACTC
Il10	TTTGAATTCCCTGGGTGAGAA and ACAGGGGAGAAATCGATGACA
Gzmb (GranzymeB)	GCTGCTCACTGTGAAGGAAGT and TGGGGAATGCATTTTACCAT
Il4	TCTCGAATGTACCAGGAGCCATATC and AGCACCTTGGAAGCCCTACAGA
Il17a	ACGCGCAAACATGAGTCCAG and CTCAGCAGCAGCAACAGCATC
Nos3as (eNOS)	CTGAGATGAGCCTCCACGCTATTTA and CAGGTGAGCCTGGCTGTGAA
Il2	GGAGCAGCTGTTGATGGACCTAC and AATCCAGAACATGCCGCAGAG
Il-12a	CCATCAGCAGATCATTCTAGACAA and CGCCATTATGATTCAGAGACTG
Ebi3 (Epstein-Barr virus induced gene 3)	GCTCCCCTGGTTACACTGAA and ACGGGATACCGAGAAGCAT
INFγ	TCAAGTGGCATAGATGTGGAAGA and TGGCTCTGCAGGATTTTCATG
Tgfb1	GTGTGGAGCAACATGTGGAACTCTA and TTGGTTCAGCCACTGCCGTA
Prf (perforin)	GCTCTTCGGGAACCAAGCTA and CAGGGTTGCTGGGCAGTG
Socs2	CGCGAGCTCAGTCAAACAG and AGTTCCTTCTGGAGCCTCTTTT
Foxp3	CCCAGGAAAGACAGCAACCTT and TTCTCACAACCAGGCCACTTG
Eos (Ikzf4)	CTCAGCACTGATGCCCAAG and CATCTCCAGGTCACGGATTT
Pde3b	GGGACTTGAAGCAGTGGTGT and TTAGCACTGAAAGATCAACTCCAT
Cd4	CAGCATGGCAAAGGTGTATTAATTAG and CCCATGCCCCTTTTTTGG